Supporting Information for

A Coumarin-Meldrum's Acid Conjugate Based Chemodosimetric Probe for Cyanide

Hongda Li,[†] Zhi Wen,[‡] Longyi Jin, [†] Yuhe Kan,*[, ‡] and Bingzhu Yin*[,†]

†Key Laboratory of Natural Resources of Changbai Mountain & Functional Molecules, Yanbian University, Ministry of Education, Yanji, Jilin 133002 , P. R. China; [‡]Jiangsu Province Key Laboratory for Chemistry of Low-Dimensional Materials, School of Chemistry and Chemical Engineering, Huaiyin Normal University, Huaian 223300

zqcong@ybu.edu.cn; yhkan@yahoo.cn

Table of Contents

1. General methods

General information and materials. Commercially available compounds were used without further purification. Solvents were dried according to standard procedures. All reactions were magnetically stirred and monitored by thin-layer chromatography (TLC) using QingDao GF254 silica gel coated plates. Fluorescence spectra were carried out on a Shimadzu RF-5301PC fluorescence spectrophotometer. UV/vis spectra were recorded with a Shimadzu UV–2550 spectrophotometer. NMR spectra were recorded on a Bruker AV-300 Spetrometer (300 MHz for ^{1}H and 75 MHz for ^{13}C), and chemical shifts were referenced relative to tetramethylsilane ($\delta_H/\delta_C = 0$). Mass data were obtained by a Shimadzu AXIMA-CFR^{TM} *plus* mass spectrometry, using a 1, 8, 9-anthracenetriol (DITH) matrix.

UV-Vis and fluorescence titration of 1 with anions. Deionized water and a spectroscopic grade of DMSO were used as the solvent for titration experiment. The titrations were carried out in 10-mm quartz cuvettes at 25 ℃. Probe **1** was dissolved in DMSO/Tris-HCl buffer (9:1, v/v, 0.01 M, pH 7.4) to afford a concentration of 5×10^{-4} M stock solution, which was diluted to 2×10^{-5} M. The different anion stock solutions of 1.0×10^{-3} M was diluted to 2.5×10^{-4} M. The absorbance was measured from 200 to 700 nm, against a blank DMSO/Tris-HCl buffer (9:1, v/v, 0.01 M, pH 7.4) solution, and different cyanide solutions were added to the 20 μM host solution (2 mL) in portions (total volume: 16, 32, 48, 64, 80, 96, 112, 128, 144, 160, 192, 224, 256, 288, 320, 400, 480, 640, 800 μL of 2.5×10^{-4} M). The emission was measured from 450 to 700 nm, and different cyanide solutions were added to the 20 μM host solution (2 mL) in portions (total volume: 16, 32, 48, 64, 80, 96, 112, 128, 144, 160, 192, 224, 256, 288, 320, 400, 480, 640, 800 μL of 2.5×10^{-4} M). The resulting solution was shaken well; the absorption and emission spectra were recorded immediately. Unless otherwise noted, for all measurements, the excitation wavelength was at 451 nm, and both the excitation and emission slit widths were 5 nm.

General procedure for ^{1}H NMR experiments. For ^{1}H NMR titrations, two stock solutions were prepared in DMSO-d_6 (5×10^{-2} M), one of them containing host only and the second one containing an appropriate concentration of guest. Aliquots of the two solutions were mixed directly in NMR tubes, which then was diluted to 0.5 mL with DMSO-d_6 if need be.

Determination of fluorescence quantum yield. Fluorescence quantum yield was determined using optically matching solutions of Rhodamine B ($\Phi_{F(S)}$ = 0.97 in ethanol and 0.001%HCl [5]) as a standard. [1-4] The quantum yield was calculated using the following equation:

$$\Phi_{F(X)} = \Phi_{F(S)} (A_S F_X / A_X F_S) (n_X / n_S)^2$$

Where Φ_F is the fluorescence quantum yield, A is the absorbance at the excitation wavelength, F is the area under the corrected emission curve, and n is the refractive index of the solvents used. Subscripts $_S$ and $_X$ refer to the standard and to the unknown, respectively.

Calculation Details. The molecular structures of the probe **1** and its cyanide adducts in the ground state optimized at the density functional theory (DFT) level using the B3LYP[6] functionals with 6-31+G(d) basis sets. The nature of all stationary points was confirmed by harmonic frequency analysis. The electronic excitation energies calculated by time-dependent DFT (TDDFT) at the B3LYP/6-31+G(d) level for the optimized ground-state structures combined with the corresponding oscillator strengths yield the UV-vis absorption spectra. Bulk solvent effects were included using linear response conductor-like polarizable continuum model (CPCM)[7,8], and DMSO was considered as solvent in analogy with the experimental medium. The molecular structures of the first singlet excited states (S_1) were optimized at the TDDFT level using the B3LYP functional with the 6-31G(d) and 6-31+G(d) basis sets. All the calculations have been performed with the GAUSSIAN09 suite of program[9].

Detection limit The detection limit was calculated based on the fluorescence titration. To determine the S/N ratio, the emission intensity of 1 (5 μM) without cyanide was measured by 10 times and the standard deviation of blank measurements was determined. Under the present conditions, a good linear relationship between the fluorescence intensity and the cyanide concentration could be obtained in the 0 - 7 μM (R = 0.996). The detection limit is then calculated with the equation: detection limit = 3σbi/m, where σbi is the standard deviation of blank measurements; m is the slope between intensity versus sample concentration. The detection limit was measured to be 34 nM at S/N = 3.

Reference

1. C. A. Parker, W. T. Rees, *Analyst*, **1960**, *85*, 587.
2. S. F. Forgues, D. Lavabre, *J. Chem. Educ.* **1999**, *76*, 1260.
3. A. Ajayaghosh, P. Carol, S. Sreejith, *J. Am. Chem. Soc.* **2005**, *127*, 14962.
4. W. Lin, L. Yuan, W. Tan, J. Feng, L. Long, *Chem. Eur. J.* **2009**, *15*, 1030.
5. T. Karstens, K. Kobs , *J. Phys. Chem.* **1980**, *84*, 1871.
6. Becke, A. D. *J. Chem. Phys.,* 1993, ***98***, 5648.
7. V. Barone, V., Cossi, M. *J. Phys. Chem. A*, 1998, **102**, 1995.
8. Cossi, M.; Rega, N.; Scalmani, G.; Barone, V. *J. Comp. Chem.*, 2003, **24,** 669-81
9. Frisch, M. J.; Trucks, G. W.; Schlegel, H. B.; Scuseria, G. E.; Robb, M. A.; Cheeseman, J. R.; Scalmani, G.; Barone, V,; Mennucci, B.; Petersson, G. A.; Nakatsuji, H.; Caricato, M.; Li, X.; Hratchian, H. P.; Izmaylov, A. F.; Bloino, J.; Zheng, G.; Sonnenberg, J. L.; Hada, M.; Ehara, M.; Toyota, K.; Fukuda, R.; Hasegawa, J.; Ishida, M.; Nakajima, T.; Honda, Y.; Kitao, O.; Nakai, H.; Vreven, T.; Montgomery, J.; J. A. , Peralta, J. E.; Ogliaro, F.; Bearpark, M.; Heyd, J. J.; Brothers, E.; Kudin, K. N.; Staroverov, V. N.; Kobayashi, R.; Normand, J.; Raghavachari, K.; Rendell, A.; Burant, J. C.; Iyengar, S. S.; Tomasi, J.; Cossi, M.; Rega, N.; Millam, J. M.; Klene, M.; Knox, J. E.; Cross, J. B.; Bakken, V.; C. Adamo, Jaramillo, J.; Gomperts, R.; Stratmann, R. E.; Yazyev, O.; Austin, A. J.; Cammi, R.; Pomelli, C.; Ochterski, J. W.; Martin, R. L.; Morokuma, K.; Zakrzewski, V. G.; Voth, G. A.; Salvador, P.; Dannenberg, J. J.; Dapprich, S.; Daniels, A. D.; Farkas, O.; Foresman, J. B.; Ortiz, J. V.; Cioslowski, J.; Fox, D. J.; Gaussian 09 Revision A.02. Gaussian.

2. Synthesis

Starting compounds **3** and **4** were synthesized according to the reported procedure [1-2].

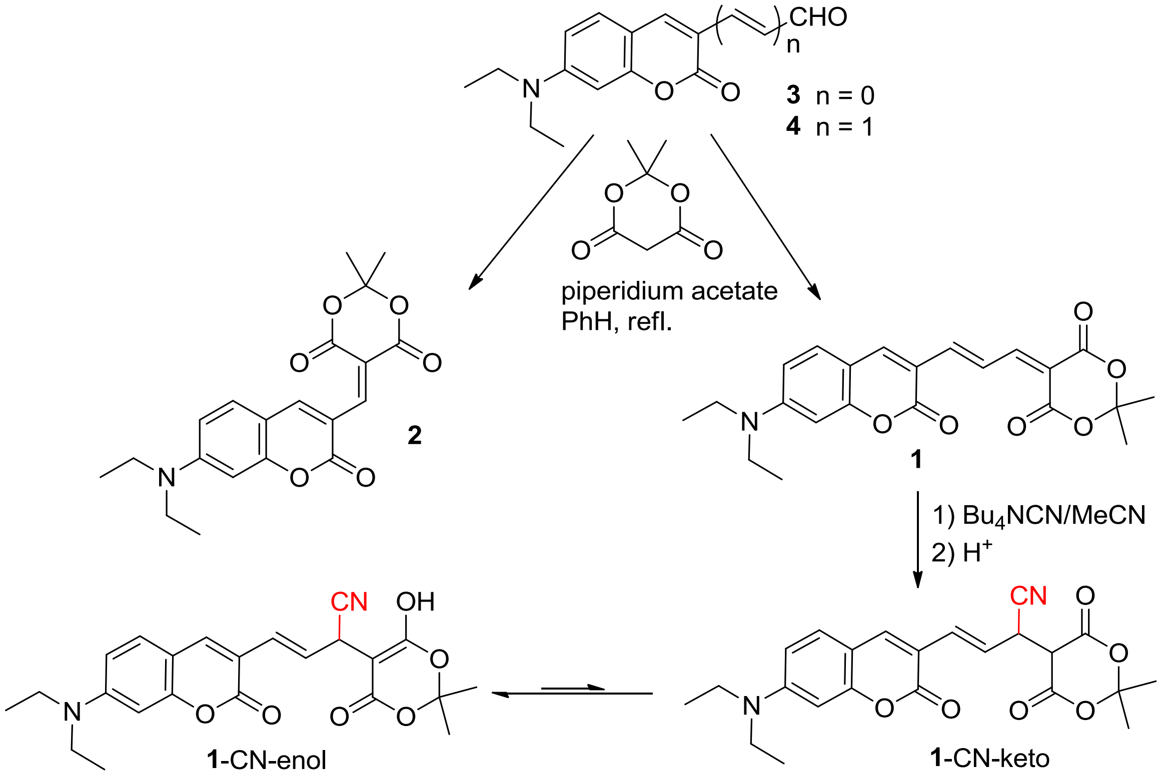

Compound 1

3-(7-(diethylamino)-2-oxo-2H-chromen-3-yl)acrylaldehyde (**4**) (135.6 mg, 0.5 mmol) and meldrum’s acid (86.5 mg, 0.6 mmol) were dissolved in dry benzene (5.0 mL). To the solution was added a 0.5M solution of pyrrolidinium acetate in benzene (200 μL) at room temperature and stirred for 1 h. The reaction mixture was diluted with EtOAc (10 mL) and washed with saturated $NaHCO_3$ solution (10 mL × 3). The organic solution was dried over $MgSO_4$ and evaporated under reduced pressure. The residue was recrystallized from MeOH to obtain the desired product **1** a purple solid 155mg (78%). Mp: 216.5-217.3 ℃. Found: C, 66.34; H, 5.55; N, 3.25 $C_{22}H_{23}NO_6$ requires C, 66.49; H, 5.83; N, 3.52. ^{1}H NMR (300 MHz, DMSO-d$_6$, ppm) δ: 8.43 (dd, *J* = 14.9 Hz, 12.5, 1H, -CH=C*H*-CH=), 8.22 (s, 1H, ArH), 8.08 (d, *J* = 12.5 Hz, 1H, =CH--C*H*=), 7.60 (d, *J* = 14.9 Hz, 1H,-C*H*=CH-), 7.58(d, *J* = 8.9 Hz, 1H, ArH), 6.80 (d, *J* = 8.9 Hz, 1H, ArH), 6.60 (s, 1H, ArH), 3.49 (q, *J* = 6.4 Hz, 4H, -C*H*$_2$-CH$_3$), 1.67 (s, 6H, -C*H*$_3$), 1.14 (t, *J* = 6.9 Hz, 6H, -CH$_2$-C*H*$_3$). ^{13}C NMR (75 MHz, DMSO-*d*$_6$, ppm) δ: 164.2, 160.6, 158.5, 153.1, 149.1, 133.1, 125.6, 115.1, 110.3, 105.7, 97.8, 46.1, 28.5, 14.0. MALDI-TOF Ms m/z: 396.30 $[M-1]^-$.

Compound 2

7-(diethylamino)-2-oxo-2H-chromene-3-carbaldehyde (**3**) (122.6 mg, 0.5 mmol) and meldrum's acid (86.5 mg, 0.6 mmol) were dissolved in dry benzene (5.0 mL). To the solution was added a 0.5M solution of pyrrolidinium acetate in benzene (200 μL) at room temperature and stirred for 1 h. The resulting solid was filtrated and washed with cold benzene. The residue was recrystallized from MeOH to obtain the desired product **2** as a red solid 148.5 mg (80%). Mp: 197.6-199.4 ℃. Found: C, 64.54; H, 5.65; N, 3.75 $C_{22}H_{23}NO_6$ requires C, 64.68; H, 570; N, 3.77. ^{1}H NMR (300 MHz, $CDCl_3$, ppm) δ: 9.45 (s, 1H, =CH-), 8.77 (s, 1H, ArH), 7.44 (d, *J* = 6.0 Hz, 1H, ArH), 6.67 (d, *J* = 6.0 Hz, 1H,ArH), 6.48(s, 1H,ArH), 3.50 (q, *J* = 7.1 Hz, $-CH_2CH_3$), 1.27 (t, *J* = 7.1 Hz, 6H, $-CH_2CH_3$). ^{13}C NMR (75 MHz, $CDCl_3$, ppm) δ: 166.2, 164.6, 162.4, 159.8, 155.2, 152.6, 151.8, 134.2, 112.4, 112.0, 110.3, 105.2, 98.2, 46.6, 28.5, 13.6. MALDI-TOF Ms m/z: 371.10 $[M]^+$.

Compound 1-CN

To a solution of compound **1** (30 mg, 0.076 mmol) in CH_2Cl_2 (3 ml) was added the Bu_4NCN (24 mg, 0.15 mmol) in CH_3CN. The resulting solution was stirred for 1 h at room temperature. The reaction mixture was acidified with 1M HCl and extracted with CH_2Cl_2. After dried over $MgSO_4$, the organic solution was evaporated under reduced pressure. The residue was purified by column chromatography on silica (from CH_2Cl_2/CH_3OH, 20:1 v/v) to give **2** (28.7 mg , 88.7%) as a yellow solid. Mp: 180.3-181.9 ℃. ^{1}H NMR (300 MHz, DMSO-*d*$_6$, ppm) δ: 7.92 (s, 1H, Ar*H*), 7.44 (d, *J* = 8.9 Hz, 1H, Ar*H*), 6.70 (d, *J* = 8.9 Hz, 1H, Ar*H*), 6.52 (br, 1H, ArH), 6.50 (d,d, *J* = 16.0, 5.9 Hz, CH=C*H*-CH), 6.40 (d, *J* = 16.0 Hz, -C*H*=CH-), 4.54 (d, *J* = 5.9 Hz,1H, -C*H*-CN), 3.43 (q, *J* = 6.8 Hz, 4H, $-CH_2-CH_3$), 1.47 (s, 6H, CH_3-), 1.12 (t, *J* = 6.8 Hz, 6H, $-CH_2-CH_3$); ^{13}C NMR (75 MHz, DMSO-d_6, ppm) δ: 165.2, 161.8, 156.7, 151.8, 140.6, 130.9, 128.7, 125.5, 122.6, 117.1, 110.7, 109.7, 101.3, 97.7, 70.6, 45.6, 32.1, 27.4, 13.9; MALDI-TOF Ms m/z: 424.50 $[M+1]^+$.

Reference

1. Wu, J.-S.; Liu, W.-X.; Zhuang, X.-Q.; Wang, F.; Wang, P.-F.; Tao, S.-L.; Zhang, X.-H.; Wu, S.-K.; Lee, S.-T. *Org. Lett.* **2007**, *9*, 33.

2. Dumas, A. M.; Seed, A. *Tetrahedron Lett.* **2007**, *48*, 7072

3. Supporting figures and tables

TableS1 Photophysical properties of probe 1 and probe 1+CN.

Compound	λ_{abs} (nm)	λ_{em} (nm)	$\varepsilon(M^{-1}cm^{-1})$	Φ_F[a]
Probe **1**	346	491	124.959	0.078
	551	641	133.257	0.083
Probe **1**+ CN	415	491	894.5	0.555

[a] λ_{ex} =451 nm

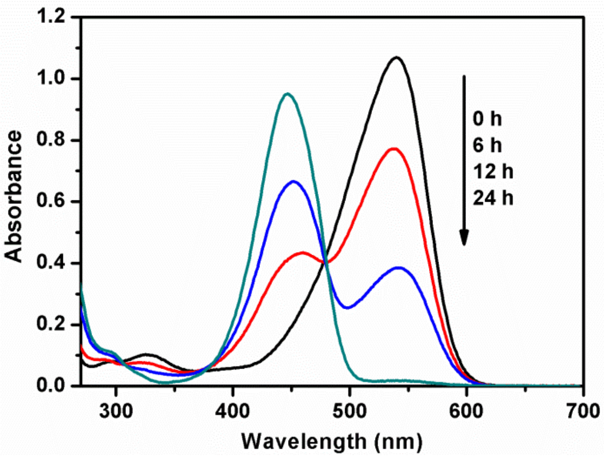

Figure S1 Time-dependant UV–vis spectral change of probe **1** (20 μM).

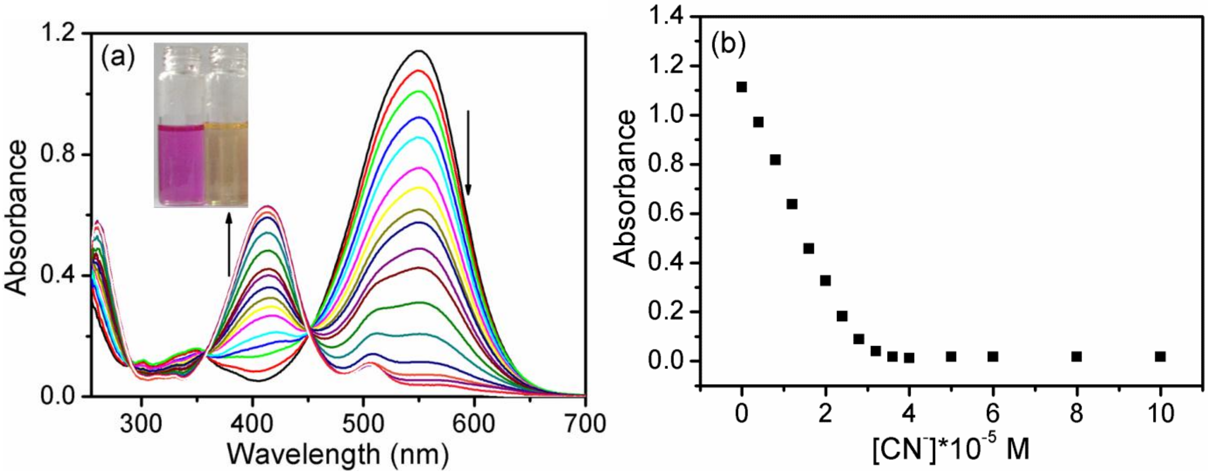

Figure S2 (a) Absorbance spectra of **1** (20 μM) in the presence of various concentrations of NaCN (0 – 5 equiv). (b) a plots of absorption 551 nm versus the equivalents of CN^- added. Inset of (a): color changes of **1** (20 μM) seen in the presence of 5 equiv of CN^-.

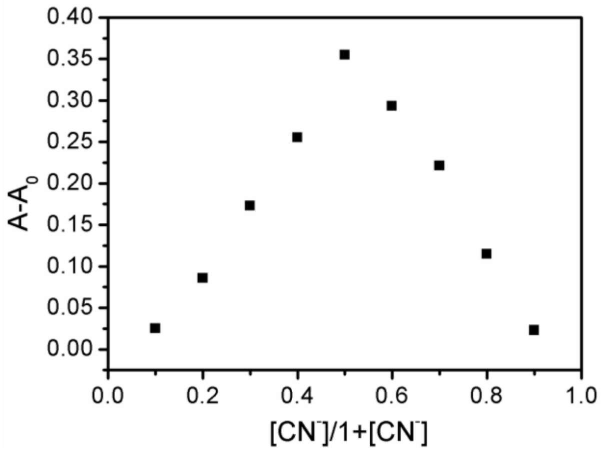

Figure S3. Job plot for **1**- CN$^-$ interaction by fluorescence response. The total molar concentration of **1** and CN$^-$ is 4×10^{-5}M.

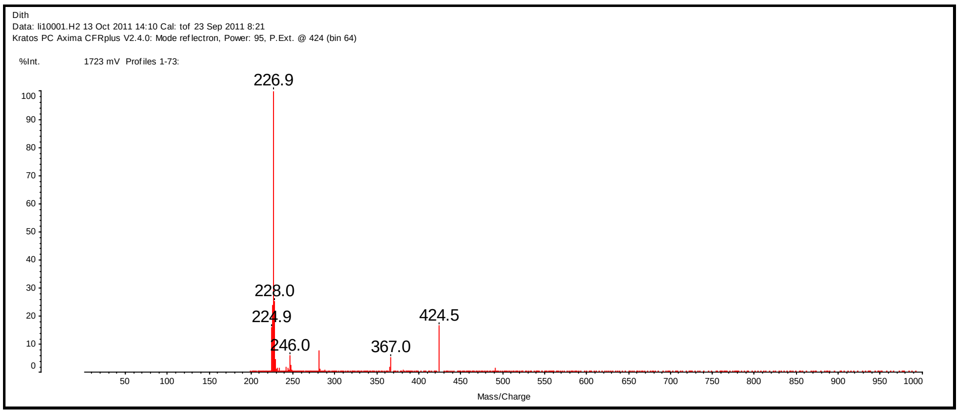
Dith
Data: li10001.H2 13 Oct 2011 14:10 Cal: tof 23 Sep 2011 8:21
Kratos PC Axima CFRplus V2.4.0: Mode reflectron, Power: 95, P.Ext. @ 424 (bin 64)

Figure S4. MALDI-TOF MS spectrum of adduct **1-CN**; $[M]^+$=424.16, Found: 424.50.

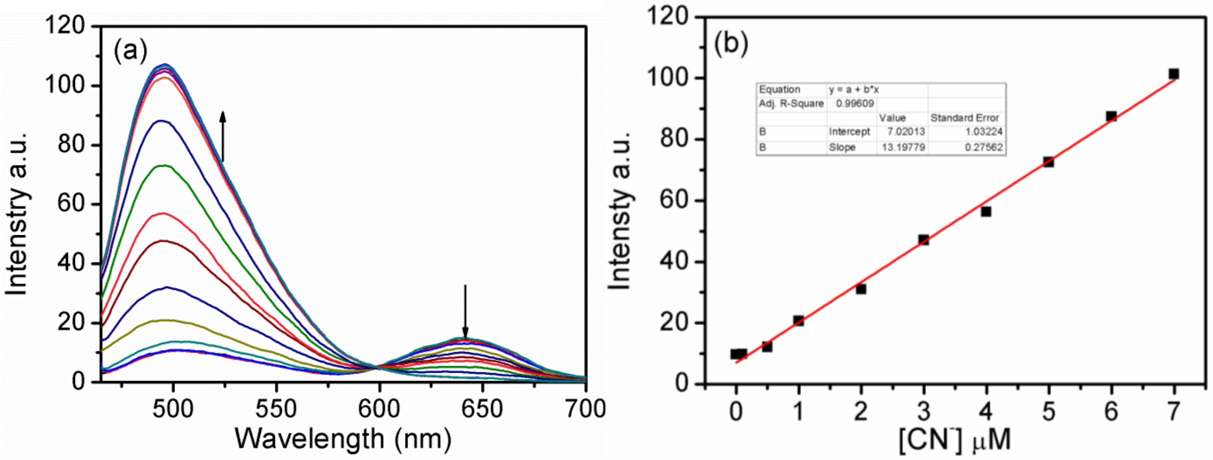

Equation	y = a + b*x		
Adj. R-Square	0.99609		
		Value	Standard Error
B	Intercept	7.02013	1.03224
B	Slope	13.19779	0.27562

Figure S5. (a) The emission spectra of **1** (5 μM) in the presence of various concentrations of NaCN (0 – 5 equiv); (b) Determination of the detection limit of CN$^-$ with **1** (5 μM) at 491 nm.

Table S2. Comparison with other methods based on Michael acceptor

Cyanide addition site	Signal to noise ratio	LOD	Selectivity	Response Time (solvent)	Reference
1. Coumarin-alkylidene-meldrum's acid	432-fold	0.04 μM	No interference	30 s (5 equiv.) (Tris-HCl, 10% DMSO)	This work
2. Coumarinyl Aldehyde	25-fold	0.10 μM	No interference	60 min (1000 equiv.) (HEPES)	7d
3 Coumarin-alkylidene-nitro group	>5-fold	3.0 μM	No interference	180 min (1 equiv.) (CH_3CN)	*
4. Calixpyrrole-alkylidene-malononitrile	No reported	No reported	Interference from halogens	No reported (CH_3CN-DMSO)	7c
5. Diphenylaminostilbene-alkylidene-malononitrile	No reported	66 μM	No interference	15 min (3 equiv.) (H_2O-THF, 40%)	**
6. Coumarin-alkylidene malononitrile	470-fold	0.80 μM	No interference	17 min (1.5 equiv.) (H_2O-THF, 50%)	7f
7. Coumarin-formylacrylonitrile	11.2-fold	0.33 μM	No interference	1 min (5 equiv.) (CH_3CN)	7e
8. Benzofurazan-alkylidene malononitrile	110-fold	1.47 μM	Interference from HS^-	2 min (5 equiv.) (H_2O-CH_3CN, 5%)	***
9. Coumarin-alkylidene-indanedione	6.5-fold	0.18 μM	No interference	35 s (2 equiv.) (CH_3CN)	****

*. Kim, G.-J.; Kim, H.-J. *Tetrahedron Lett*. **2010**, 51, 185

. Lin, Y.-D.; Peng, Y.-S.; Su, W.; Tu, C.-H.; Sun, C.-H.; Chow, T. J. *Tetrahedron* **2012, 68, 2523.

*** Liu, Z.; Wang, X.; Yang, Z.; He, W. *J. Org. Chem*. **2011**, 76, 10286.

**** Zhou, X.; Lv, X.; Hao, J.; Liu D.; Guo, W. *Dyes Pigm*. **2012**, 95, 168.

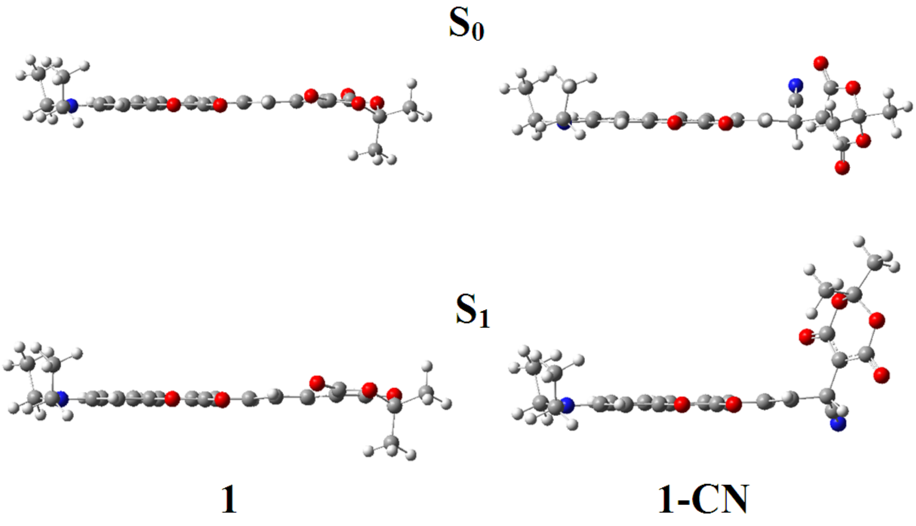

Figure S6. Optimized structures of **1** and **1-CN** at the ground state (S_0) and the first excited state (S_1)

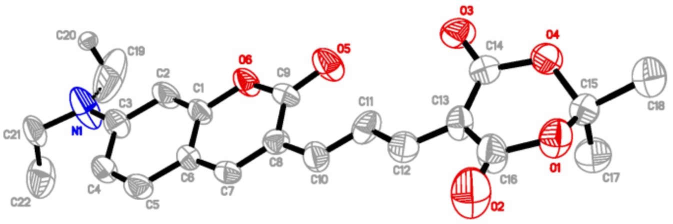

Figure S7. X-ray crystal structure of **1**. All hydrogen atoms are omitted for clarity. The thermal ellipsoids are shown at the 30% probability level.

Table S3 Crystal data and structure refinements for compound **1.**

Empirical formula	C22 H23 N O6
Formula weight	397.41
Temperature	293(2) K
Wavelength	0.71073 A
Crystal system	monoclinic
Space group	C 2/c
a (Å)	27.689 (5)
b (Å)	7.9853 (16)
c (Å)	18.998 (4)
α (^{o})	90
β (^{o})	93.73 (3)
γ (^{o})	90
V (Å^3)	4191.7 (14)
Z	8
$D_{calc.}$(g cm^{-3})	1.259
Abs coeff. (mm^{-1})	0.09
F(000)	1680
R(int)	0.225
GOOF on F^2	0.903
Final R indices [I>2sigma(I)]	[a]R1 = 0.0951, [b]R_w = 0.2325
R indices (all data)	[a]R1 = 0.2751, [b]R_w = 0.3556

[a] $R1 = ||F_o| - |F_c||/|F_o|$. [b] $R_w = [w(F_o^2 - F_c^2)^2/w(F_o^2)^2]^{1/2}$.

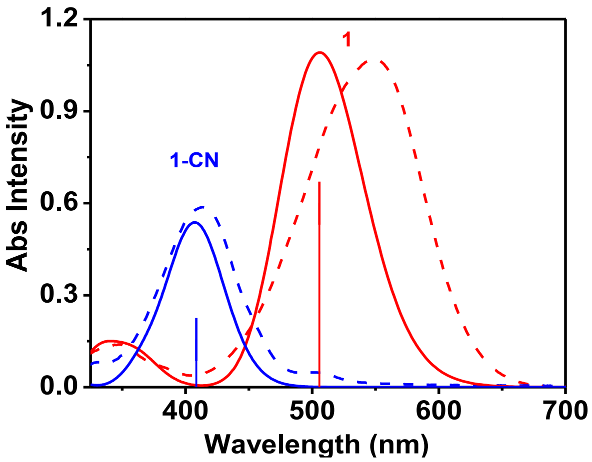

Figure S8. Experimental absorption spectra (dash) of probe **1** and their cyanide adducts compared with calculated spectra (solid) in DMSO solvent with TD-CPCM-B3LYP methods at 6-31+G(d) basis set.

Table S4. Calculated and experimental absorption (nm, eV in parenthesis), oscillator strength (*f*) and transition nature of probe **1** and their cyanide adducts **1-CN** in DMSO solvent with various functional at 6-31+G(d) basis set.

	State	λ_{max}(nm/eV)	*f*	Transition contributions	expt.
		1			
B3LYP	$S_0 \rightarrow S_1$	505.7(2.45)	1.6315	HOMO→LUMO(100%)	550
CAM-B3LYP	$S_0 \rightarrow S_1$	445.6(2.78)	1.9264	HOMO→LUMO(91%)	
		1-CN$^-$			
B3LYP	$S_0 \rightarrow S_1$	408.6(3.03)	0.7702	HOMO→LUMO(94%)	413
CAM-B3LYP	$S_0 \rightarrow S_1$	359.2(3.45)	1.1170	HOMO→LUMO(94%)	

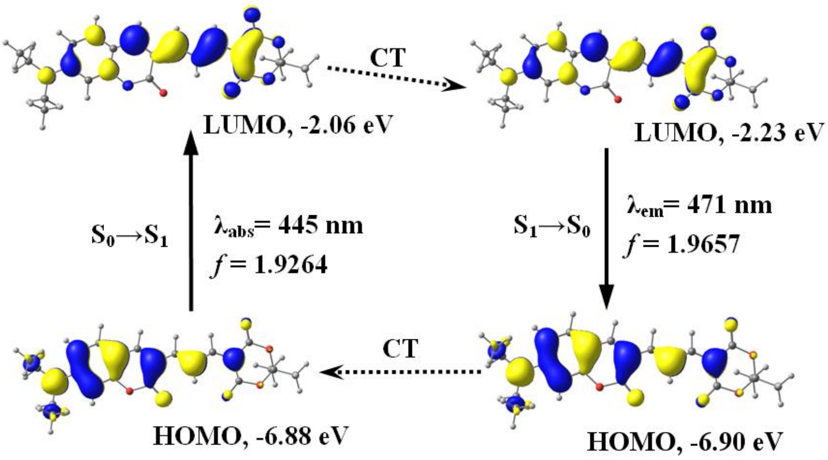

Figure S9. The frontier MOs involved in the vertical excitation and the emission of probe **1**. The vertical absorption and emission energies calculation were performed by TD-B3LYP/6-31+G* based on the ground state (S_0) geometry and lowest-lying singlet excited state (S_1) geometry optimized at at B3LYP/6-31+G* and TD-B3LYP /6-31+G* level of theory, respectively. DMSO was used as solvent in the calculation. CT stands for conformation transformation.

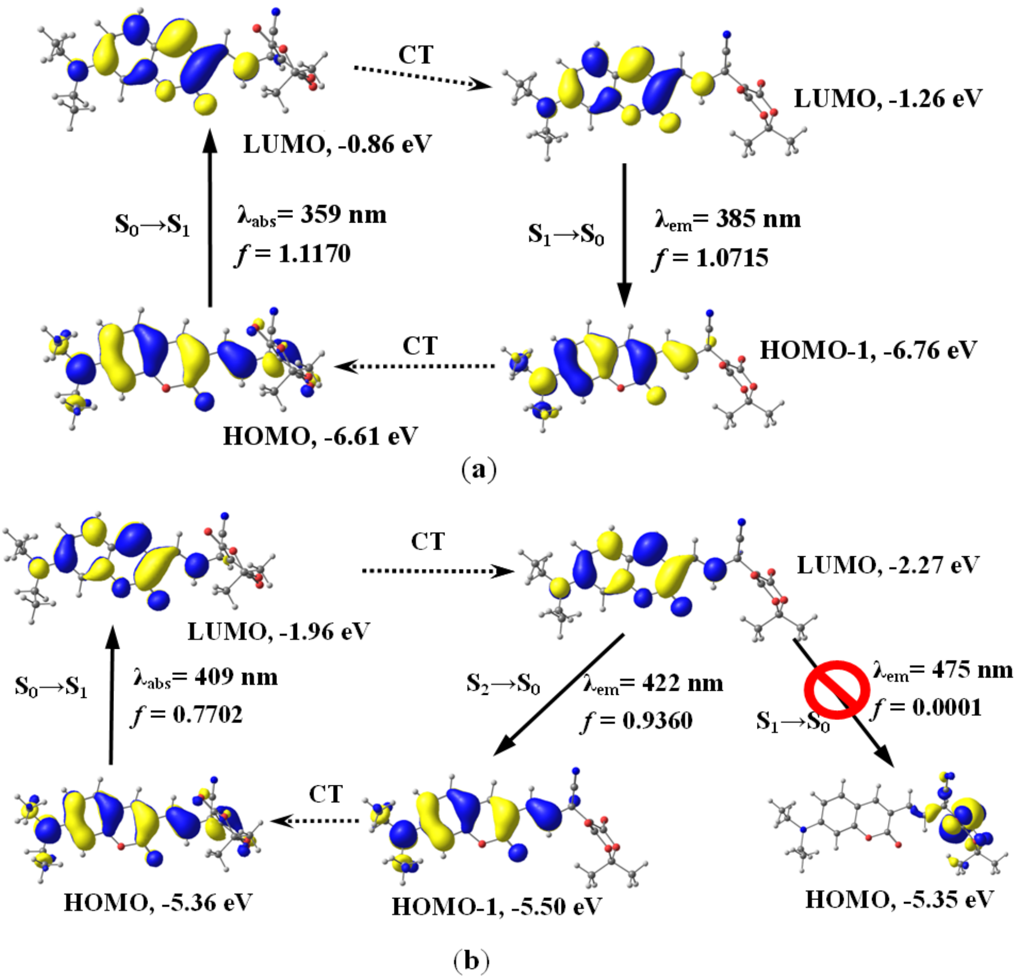

Figure S10. The frontier MOs involved in the vertical excitation and the emission of **1-CN**. The vertical absorption and emission energies calculation were performed by (**a**) TD-B3LYP/6-31+G*, (**b**) TD-B3LYP/6-31+G* based on the ground state (S_0) geometry and lowest-lying singlet excited state (S_1) geometry optimized at at B3LYP/6-31+G* and TD-B3LYP/6-31G* level of theory, respectively. DMSO was used as solvent in the calculation.

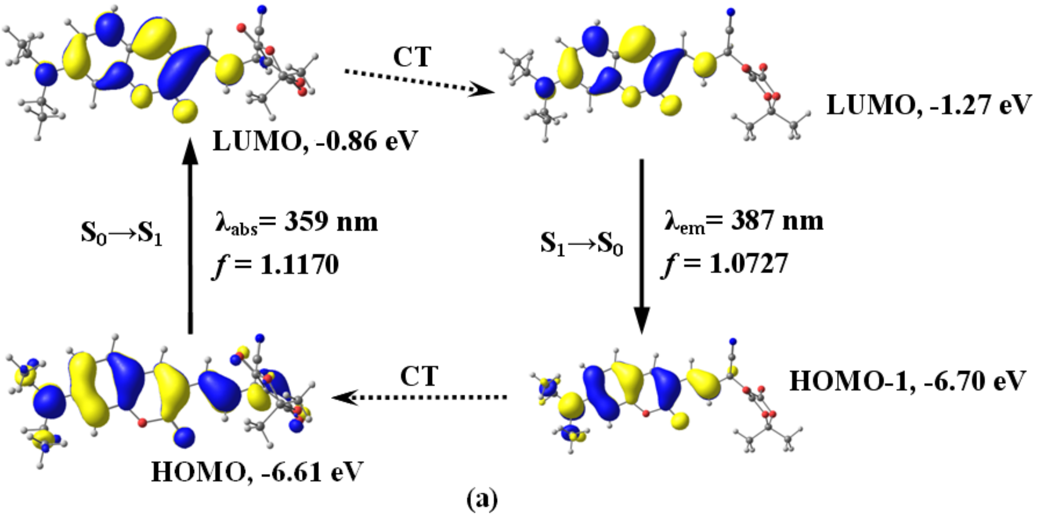

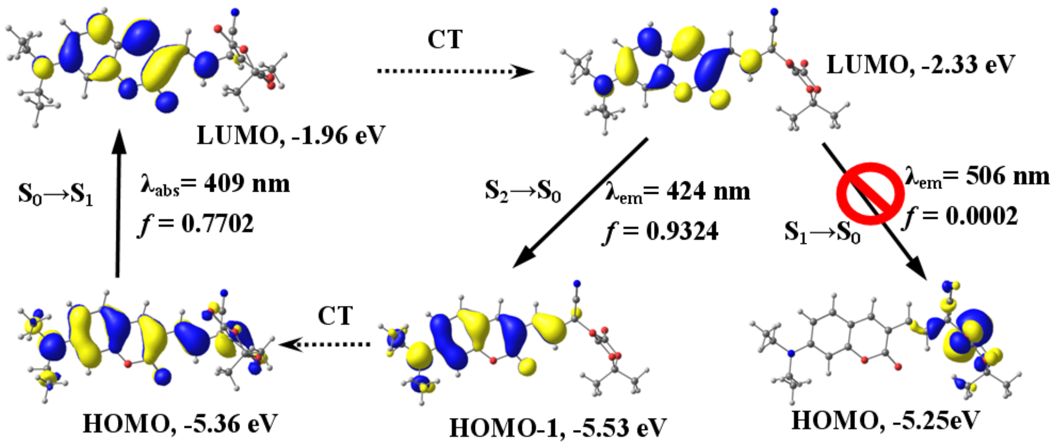

(b)

Figure S11. The frontier MOs involved in the vertical excitation and the emission of **1-CN**. The vertical absorption and emission energies calculation were performed by (**a**) TD-B3LYP/6-31+G*, (**b**) TD-B3LYP/6-31+G* based on the ground state (S_0) geometry and lowest-lying singlet excited state (S_1) geometry optimized at B3LYP/6-31+G* and TD-B3LYP/6-31+G* level of theory, respectively. DMSO was used as solvent in the calculation.

Table S5. Calculated emission energies (nm, eV in parenthesis), oscillator strength (*f*) and transition nature of probe **1** and their cyanide adducts **1-CN** in DMSO solvent with TDDFT/6-31+G(d) level of theory at based on S_1 geometry optimized by TD-B3LYP/6-31G*

Functional	state	Emission energy	*f*	Transition nature	Exp.
		1			
PBE	$S_1 \rightarrow S_0$	622.3(1.99)	1.0662	LUMO→HOMO (96%)	641
B3LYP	$S_1 \rightarrow S_0$	528(2.35)	1.4587	LUMO→HOMO (100%)	
PBE0	$S_1 \rightarrow S_0$	509.2(2.43)	1.5506	LUMO→HOMO (99%)	
BHandHLYP	$S_1 \rightarrow S_0$	438.8(2.83)	1.8828	LUMO→HOMO (92%)	
M06-2X	$S_1 \rightarrow S_0$	460.2(2.69)	1.7879	LUMO→HOMO (91%)	
CAM-B3LYP	$S_1 \rightarrow S_0$	451.5(2.75)	1.8283	LUMO→HOMO(88%)	
LC-ωPBE	$S_1 \rightarrow S_0$	413.6(3.00)	1.9358	LUMO→HOMO(77%)	
		1-CN$^-$			
BP86	$S_1 \rightarrow S_0$	793.8(1.56)	0.0000	LUMO→HOMO(100%)	492
	$S_2 \rightarrow S_0$	473.0(2.62)	0.7237	LUMO→HOMO-1(96%)	
B3LYP	$S_1 \rightarrow S_0$	475.2(2.60)	0.0001	LUMO→HOMO(92%)	
	$S_2 \rightarrow S_0$	421.7(2.94)	0.9360	LUMO→HOMO-1(82%)	
PBE0	$S_1 \rightarrow S_0$	464.8(2.68)	0.0001	LUMO→HOMO(100%)	
	$S_2 \rightarrow S_0$	410.5(3.02)	0.9860	LUMO→HOMO-1(99%)	
BHandHLYP	$S_1 \rightarrow S_0$	374.5(3.31)	1.1247	LUMO→HOMO(96%)	
M06-2X	$S_1 \rightarrow S_0$	385.7(3.21)	1.1009	LUMO→HOMO-1(97%)	
CAM-B3LYP	$S_1 \rightarrow S_0$	384.8(3.22)	1.0715	LUMO→HOMO-1(96%)	
LC-BP86	$S_1 \rightarrow S_0$	358.9(3.45)	1.1552	LUMO→HOMO (92%)	
LC-ωPBE	$S_1 \rightarrow S_0$	364.4(3.40)	1.1241	LUMO→HOMO (92%)	
ωB97XD	$S_1 \rightarrow S_0$	382.0(3.25)	1.0741	LUMO→HOMO-1(96%)	

Table S6. Calculated emission energies (nm, eV in parenthesis), oscillator strength (*f*) and transition nature of probe **1** and their cyanide adducts **1-CN** in DMSO solvent with TD-CPCM-DFT/6-31+G(d) level of theory at based on TD-B3LYP/6-31+G* optimized S_1 geometry

Functional	state	Emission energy	*f*	Transition nature	Exp.
		1			
mPWPW91	$S_1 \rightarrow S_0$	589.6(2.10)	1.3426	LUMO→HOMO (97%)	641
PBE	$S_1 \rightarrow S_0$	589.7(2.10)	1.3464	LUMO→HOMO(97%)	
B3LYP	$S_1 \rightarrow S_0$	521.5(2.38)	1.7335	LUMO→HOMO(97%)	
PBE0	$S_1 \rightarrow S_0$	507.7(2.44)	1.8078	LUMO→HOMO(97%)	
M06-2X	$S_1 \rightarrow S_0$	478.8(2.59)	1.9420	LUMO→HOMO(94%)	
CAM-B3LYP	$S_1 \rightarrow S_0$	470.6(2.63)	1.9657	LUMO→HOMO(92%)	
LC-ωPBE	$S_1 \rightarrow S_0$	444.0(2.79)	2.0196	LUMO→HOMO(84%)	
		1-CN			
mPWPW91	$S_1 \rightarrow S_0$	811.6 (1.53)	0.0002	LUMO→HOMO (100%)	492
	$S_2 \rightarrow S_0$	475.8(2.61)	0.7209	LUMO→HOMO-1(96%)	
PBE	$S_1 \rightarrow S_0$	814.9(1.52)	0.0002	LUMO→HOMO (100%)	
	$S_2 \rightarrow S_0$	475.8(2.60)	0.7230	LUMO→HOMO-1(96%)	
B3LYP	$S_1 \rightarrow S_0$	506.6(2.45)	0.0002	LUMO→HOMO(100%)	
	$S_2 \rightarrow S_0$	424.0(2.92)	0.9324	LUMO→HOMO-1(99%)	
PBE0	$S_1 \rightarrow S_0$	469.3(2.64)	0.0005	LUMO→HOMO(99%)	
	$S_2 \rightarrow S_0$	412.5(3.01)	0.9860	LUMO→HOMO-1(99%)	
M06-2X	$S_1 \rightarrow S_0$	387.7(3.19)	1.1023	LUMO→HOMO-1(97%)	
CAM-B3LYP	$S_1 \rightarrow S_0$	386.7(3.21)	1.0727	LUMO→HOMO-1(96%)	
LC-ωPBE	$S_1 \rightarrow S_0$	366.2(3.39)	1.1266	LUMO→HOMO-1(91%)	

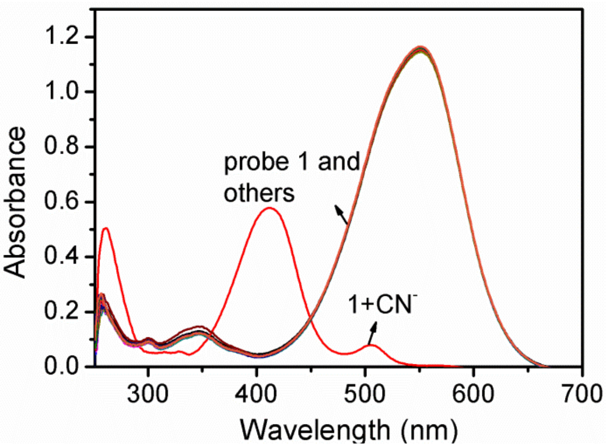

Figure S12 Absorption spectra of **1** (20 μM) in the presence of various relevant analytes. (5 equiv of CN^-, F^-, AcO^-, $H_2PO_4^-$, HSO_4^-, ClO_4^-, Cl^-, Br^-, I^-, NO_2^-, NO_3^-, N_3^-, S^{2-} and L-cys, Hcy, GSH.)

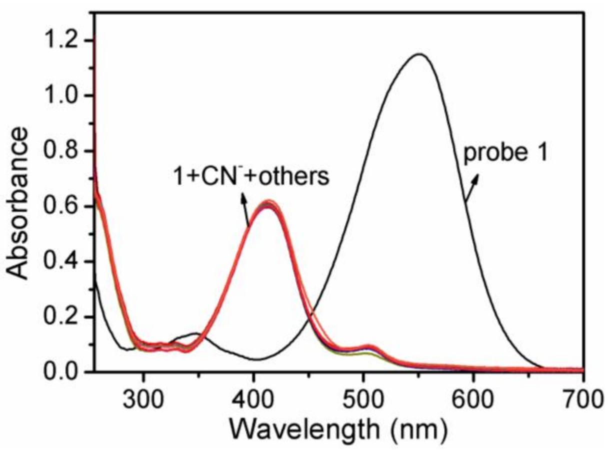

Figure S13. The absorption spectra of probe **1** (20 μM) to CN^- anions in the presence of various interfering analytes (5 equiv of CN^-, F^-, AcO^-, $H_2PO_4^-$, HSO_4^-, ClO_4^-, Cl^-, Br^-, I^-, NO_2^-, NO_3^-, N_3^-, S^{2-} and L-cys, Hcy, GSH.)

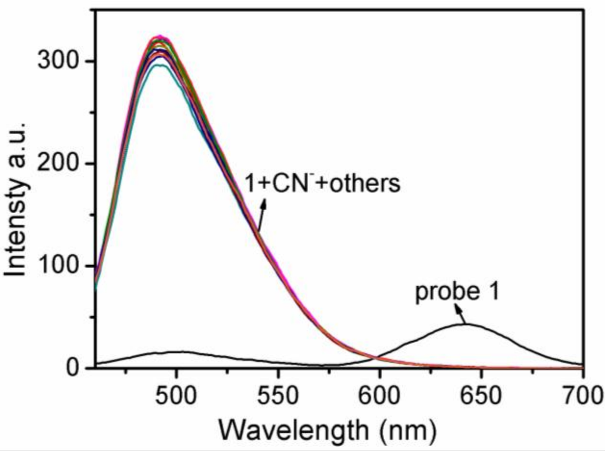

Figure S14. The emission spectra of probe **1** (20 μM) to CN^- anions in the presence of various interfering analytes (5 equiv of CN^-, F^-, AcO^-, $H_2PO_4^-$, HSO_4^-, ClO_4^-, Cl^-, Br^-, I^-, NO_2^-, NO_3^-, N_3^-, S^{2-} and L-cys, Hcy, GSH.). λ_{ex} = 451 nm, λ_{em} = 491 nm.

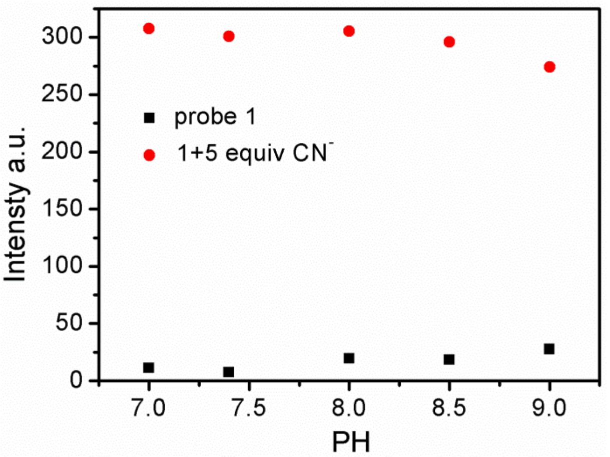

Figure S15. The fluorescence intensity of probe **1** (20 μM) in the absence (■) and in the presence (●) of 5 equiv of CN^- at different pH values. λ_{ex} = 451 nm, λ_{em} = 491 nm.

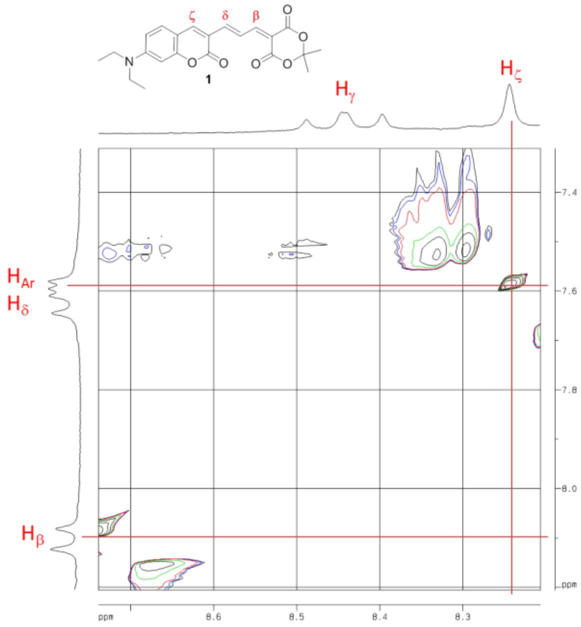

Figure S16. 2D NOESY spectrum of probe **1** in DMSO at 298.1 K with a mixing time of 800 ms.

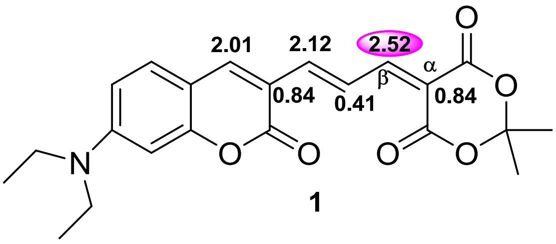

Figure S17. The electrophilic Fukui function for the probe **1** in DMSO solvent with B3LYP/6-31+G(d) method.

.

4. Characteration data

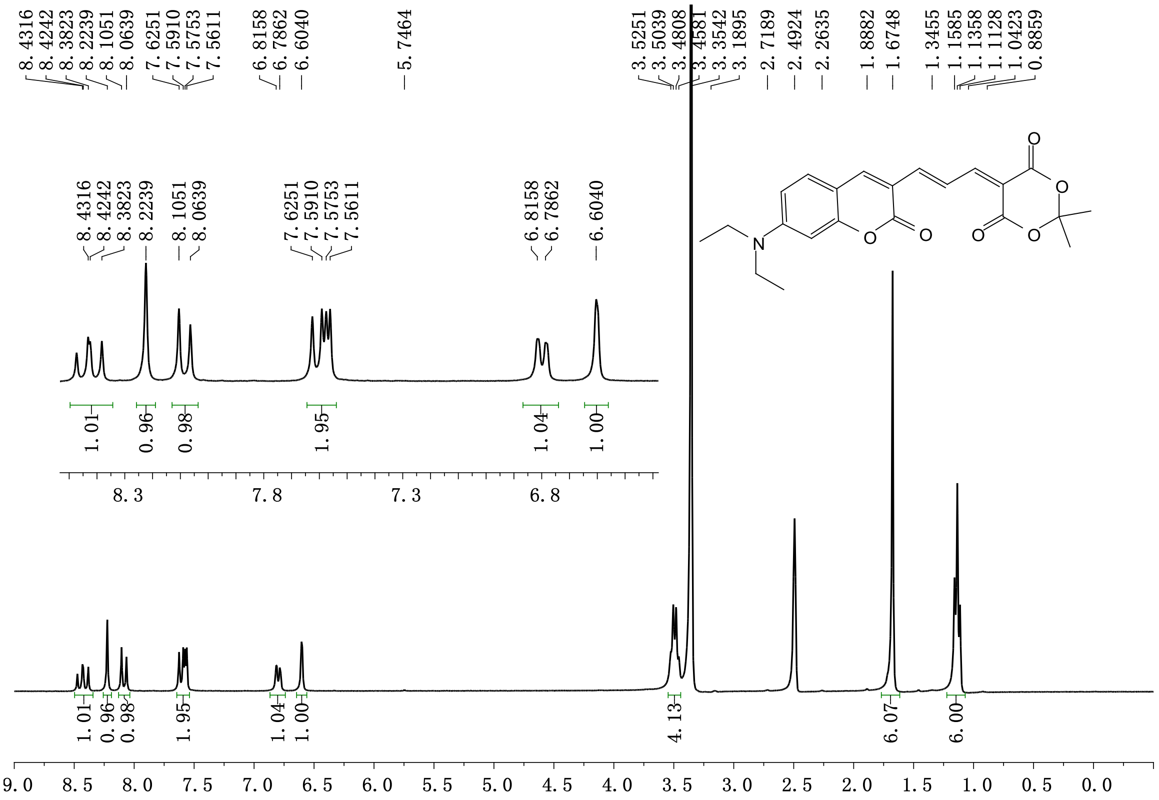

Figure S20. ^{1}H NMR spectrum of compound **1** in DMSO-d_6.

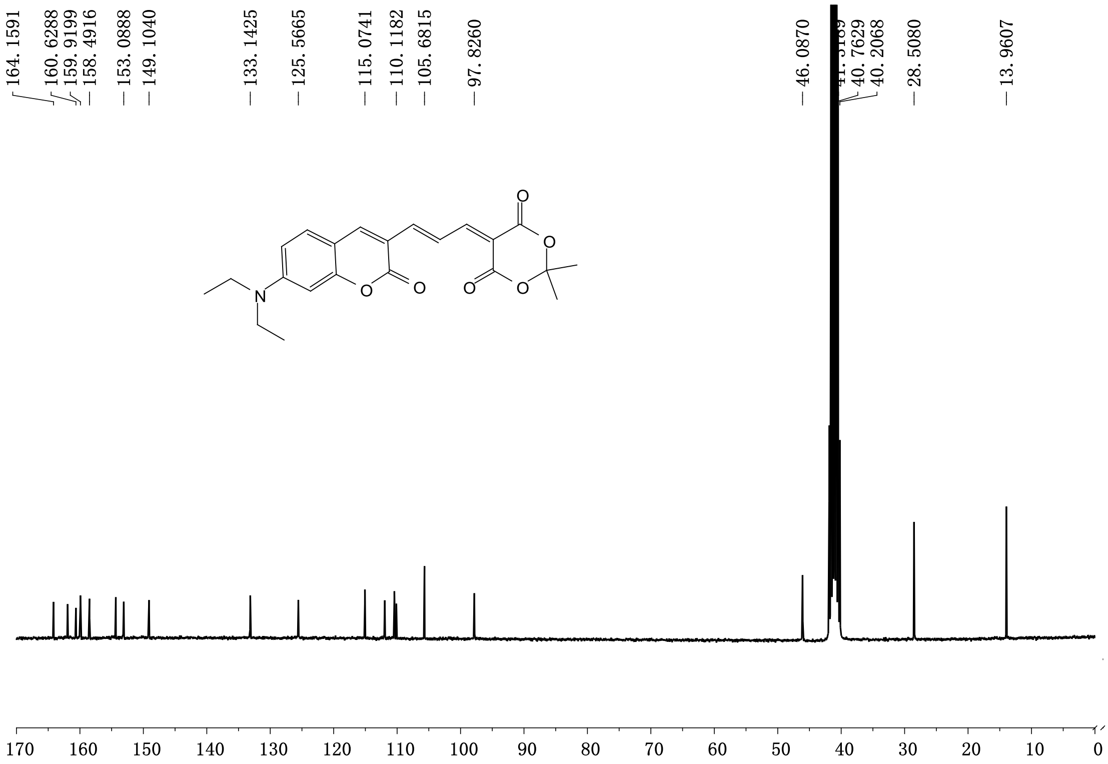

Figure S21. ^{13}C NMR spectrum of compound **1** in DMSO-d_6.

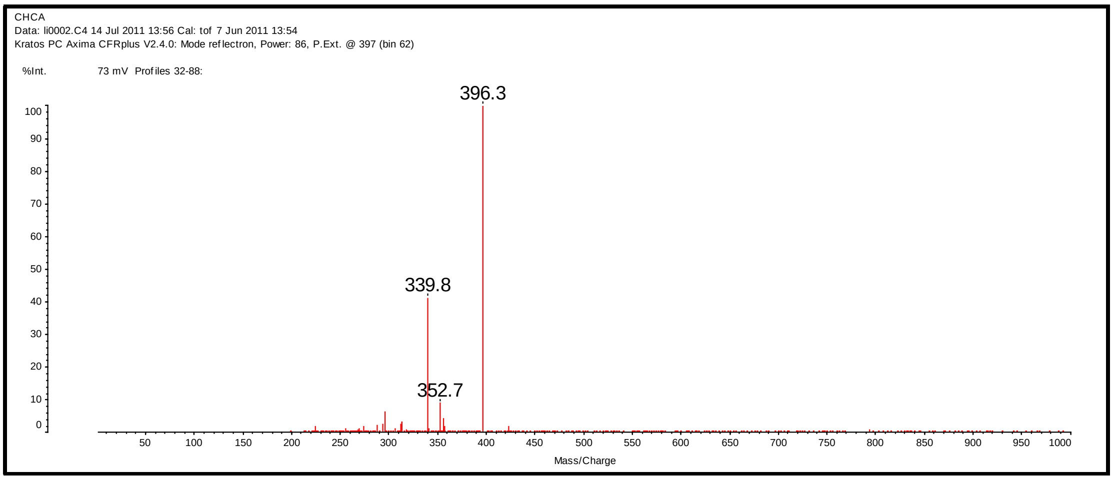

Figure S22. MALDI-TOF MS spectrum of compound **1** (M$^+$=397.15, Found: 396.3([M-H]$^+$).

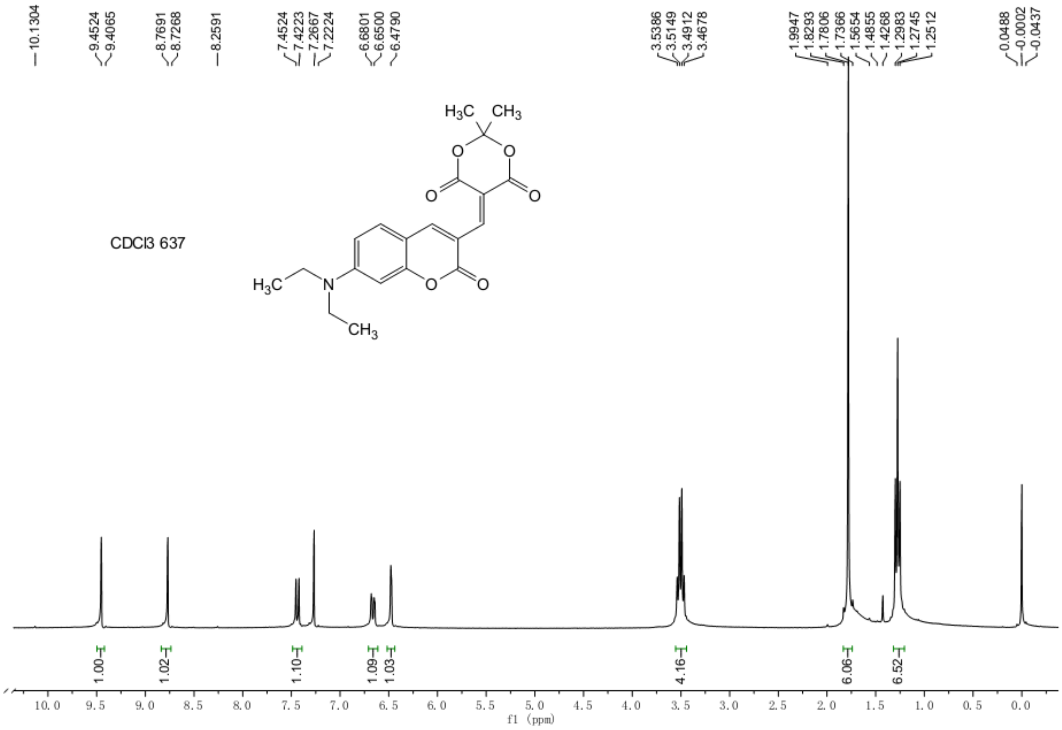

Figure S23. ^{1}H NMR spectrum of compound **2** in $CDCl_3$

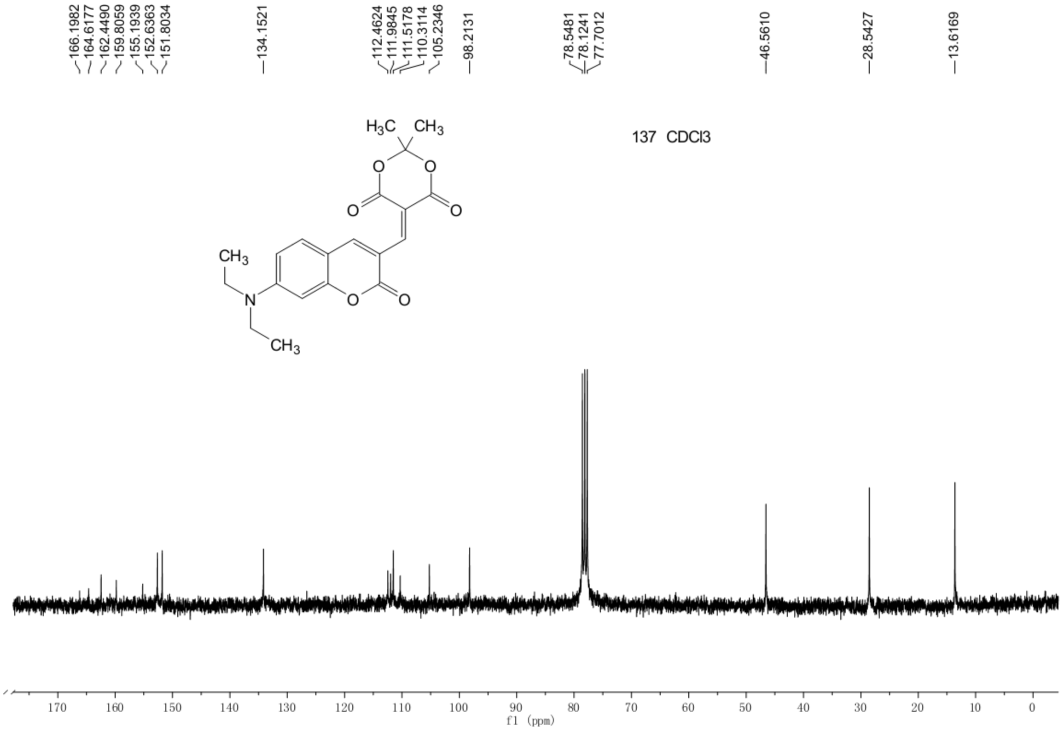

Figure S24 ^{13}C NMR spectrum of compound **2** in $CDCl_3$.

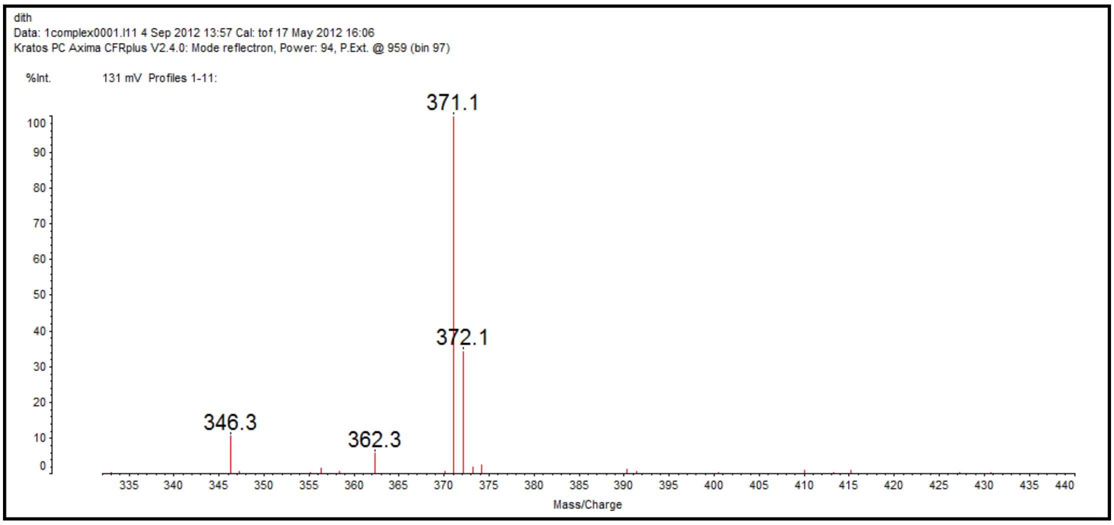

Figure S25. MALDI-TOF MS spectrum of adduct **2.** $[M]^+$=371.14, Found: 371.10.

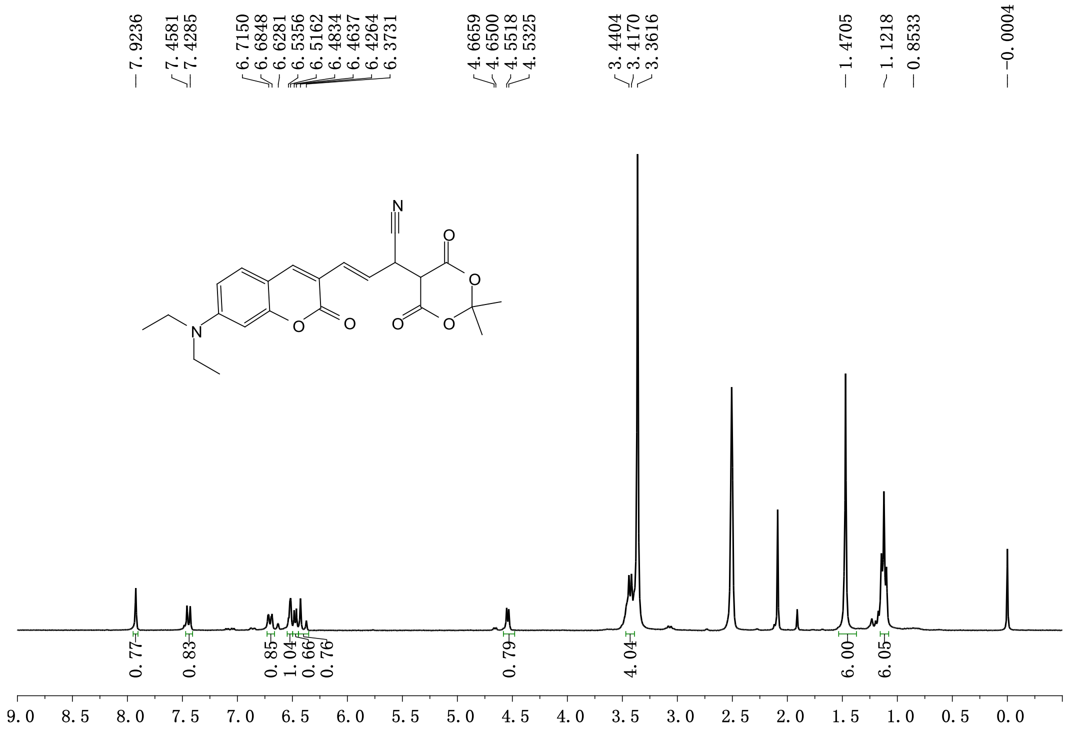

Figure S26. ^{1}H NMR spectrum of compound **1-CN** in DMSO-d_6..

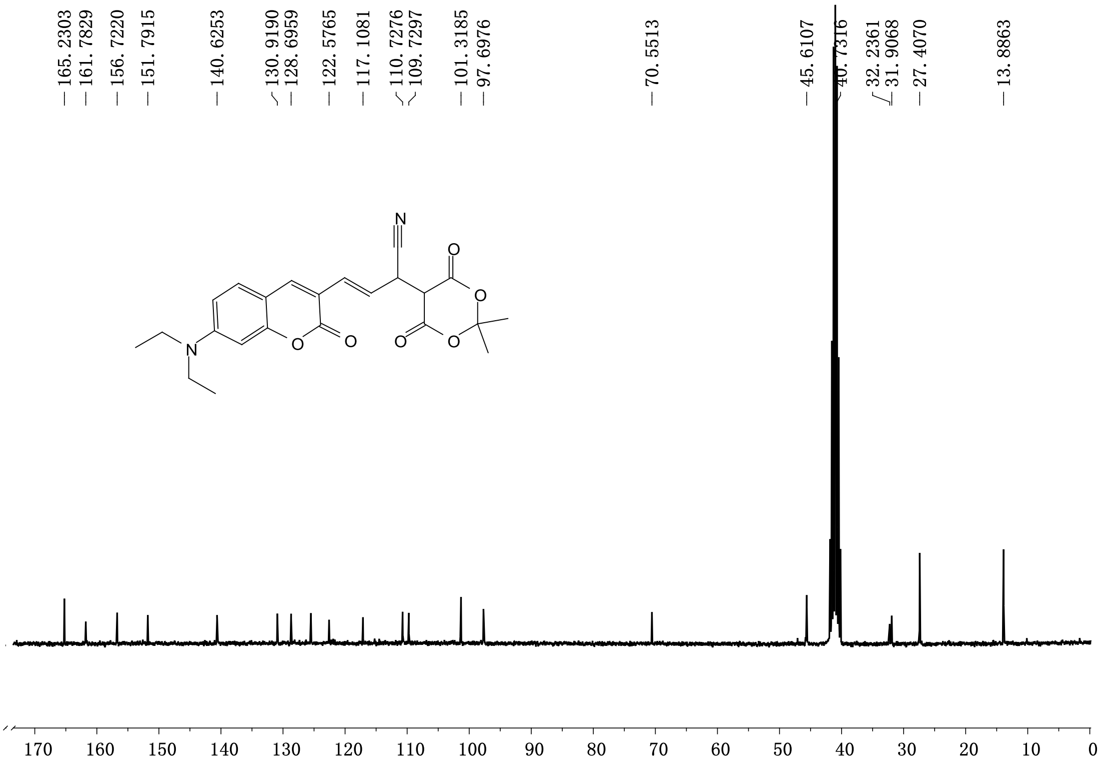

Figure S27. ^{13}C NMR spectrum of compound **1-CN** in DMSO-d_6.